

Low mass Drell-Yan production at the CERN LHC within the dipole formalism ¹

Maria Beatriz Gay Ducati

*Universidade Federal do Rio Grande do Sul.
Programa de Pós-Graduação em Física.
Grupo de Fenomenologia de Partículas de Altas Energias.*

¹Based on Ref: arXiv:1307.6882v1 [hep-ph] M.B. Gay Ducati, M.T. Griep and M.V.T. Machado

- Introduction;
- Dileptons production in high energies;
- Dipoles formalism for the Drell- Yan;
- Results for the dileptons production;
- Conclusion.

- The study of DY cross section with dileptons carrying large values of p_T is an important probe of short-distance hadron dynamics;
- Production of dileptons in DY process can help to constraint the parton distribution functions (PDFs);
- The dileptons can be a powerful probe of the initial state of matter created in heavy ion collisions;
- Those electromagnetic probes are crucial to determine the dominant physics in the forward region at RHIC and at the LHC;

Dileptons Production in high energies

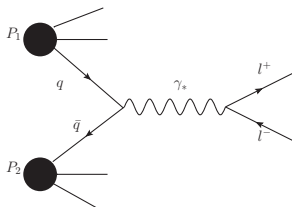


Figure: Drell-Yan process in LO in QCD.

In the D.Y. process the transfer momentum is the invariant mass of the lepton pair in the final state, and corresponds to the process scale. So,

$$M^2 = q^2 > 0 \quad (1)$$

where q^μ is the quadrimomentum of the virtual foton. The center of mass energy square of the colliding hadrons is given by:

$$s = (P_1 + P_2)^2 \quad (2)$$

where P_1 e P_2 are the quadrimomenta of the hadron 1 and hadron 2, respectively.

Dileptons Production in high energies

A useful variable to work with DY processes with fixed target is the fraction of the total longitudinal momentum, known as Feynman x_F , defined as:

$$x_F = \frac{2p_L}{\sqrt{s}} \approx x_1 - x_2 \quad (3)$$

where p_L is the longitudinal momentum of the leptons pair, in the hadron-hadron center of mass frame, and x_1 and x_2 are the momentum fraction carried by the partons. So:

$$p_1 = x_1 P_1 \quad \text{and} \quad p_2 = x_2 P_2 \quad (4)$$

where p_1 and p_2 are the momenta carried by the partons. So, we can write:

$$x_1 = \frac{2P_2 \cdot q}{s} \quad \text{and} \quad x_2 = \frac{2P_1 \cdot q}{s} \quad (5)$$

In addition, the variables x_1 e x_2 are related by:

$$\tau = x_1 x_2 = \frac{M^2}{s} \quad (6)$$

where the foton virtual transverse momentum was neglected.

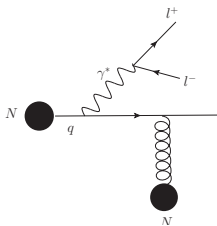


Figure: A quark or antiquark of the projectile scatters with the color field of the target and radiates a photon (before or after scattering), which decays as a leptons pair.

In the dipoles formalism, the cross section for radiation of a virtual photon from a quark scattering from a nucleon (N) can be written as:

$$\frac{d\sigma_{T,L}(qN \rightarrow \gamma^* X)}{d \ln \alpha} \int d^2 r_{\perp} |\Psi_{\gamma^* q}^{T,L}(\alpha, r_{\perp})|^2 \sigma_{dip}(\alpha r_{\perp}) \quad (7)$$

and that the wave functions are given by:

$$|\Psi_{\gamma^* q}^{T,L}(\alpha, r_{\perp})|^2 = |\Psi_{\gamma^* q}^T(\alpha, r_{\perp})|^2 + |\Psi_{\gamma^* q}^L(\alpha, r_{\perp})|^2, \quad (8)$$

$$|\Psi_{\gamma^* q}^T(\alpha, r_{\perp})|^2 = \frac{\alpha_{em}}{\pi^2} \{m_f^2 \alpha^4 K_0^2(\eta r_{\perp}) + [1 + 1 - \alpha] \eta K_1^2(\eta r_{\perp})\}, \quad (9)$$

$$|\Psi_{\gamma^* q}^L(\alpha, r_{\perp})|^2 = \frac{2\alpha_{em}}{\pi^2} M^2 (1 - \alpha) K_0^2(\eta r_{\perp}) \quad (10)$$

where $\eta = \alpha(1 - \alpha)M^2 + m_f^2$, K_0 and K_1 are the modified Bessel functions.

In the dipoles formalism, the D.Y. transverse momentum distribution is given by:

$$\begin{aligned}
 \frac{d^3\sigma(pp \rightarrow l^+l^- X)}{dy dM^2 dp_T^2} &= \frac{\alpha_{em}}{3M^2} x_1 \int_{x_1}^{\alpha_{max}} \frac{d\alpha}{\alpha} \sum_{q=1}^{N_f} e_q^2 \left[q \left(\frac{x_1}{\alpha} \right) + \bar{q} \left(\frac{x_1}{\alpha} \right) \right] \\
 &\times \int d^2r_{\perp} d^2r'_{\perp} e^{i\vec{p}_T(\vec{r}_{\perp} - \vec{r}'_{\perp})} [\psi_{\gamma^*q}^T(\alpha, r_{\perp}) \Psi_{\gamma^*q}^{T*}(\alpha, r'_{\perp}) + \psi_{\gamma^*q}^L(\alpha, r_{\perp}) \Psi_{\gamma^*q}^{L*}(\alpha, r'_{\perp})] \\
 &\times \frac{1}{2} [\sigma_{dip}(x, \alpha r_{\perp}) + \sigma_{dip}(x, \alpha r'_{\perp}) - \sigma_{dip}(x, \alpha |\vec{r}_{\perp} - \vec{r}'_{\perp}|)]
 \end{aligned} \tag{11}$$

Dipoles formalism for the Drell-Yan

What can be rewritten as:

$$\frac{d\sigma^{DY}}{dM^2 dx^F dp_T^2} = \frac{\alpha_{em}^2}{6\pi^3 M^2} \frac{1}{(x_1 + x_2)} \int d\rho W(\rho, p_T) \sigma_{dip}(\rho) \quad (12)$$

with the weight function $W(\rho, p_T)$, given by:

$$\begin{aligned} W(\rho, p_T) = & \int_{x_1}^{\alpha_{max}} \frac{d\alpha}{\alpha} \sum_{q=1}^{N_f} e_q^2 \left[q \left(\frac{x_1}{\alpha} \right) + \bar{q} \left(\frac{x_1}{\alpha} \right) \right] \\ & \times \left\{ \left[m_q^2 \alpha^4 + 2M^2 (1 - \alpha)^2 \right] \left[\frac{1}{\rho_T^2 + \eta^2} T_1(\rho) - \frac{1}{4\eta} T_2(\rho) \right] \right. \\ & \left. + [1 + (1 - \alpha)^2] \left[\frac{\eta p_T}{\rho_T^2 + \eta^2} T_3(\rho) - \frac{T_1(\rho)}{2} + \frac{\eta}{4} T_2(\rho) \right] \right\} \quad (13) \end{aligned}$$

with

$$T_1(\rho) = \rho J_0(p_T \rho / \alpha) K_0(\eta \rho / \alpha) / \alpha \quad (14)$$

$$T_2(\rho) = \rho^2 J_0(p_T \rho / \alpha) K_1(\eta \rho / \alpha) / \alpha^2 \quad (15)$$

$$T_3(\rho) = \rho J_1(p_T \rho / \alpha) K_1(\eta \rho / \alpha) / \alpha \quad (16)$$

Drell-Yan differential cross section

We calculate the differential cross section for the Drell-Yan production, given by:

$$\begin{aligned} \frac{d\sigma(pp \rightarrow \gamma X)}{dM dy dp_T^2} &= \frac{\alpha_{em}}{12\pi^3 M^2} \int_{x_1}^{\alpha_{max}} \frac{d\alpha}{\alpha} F_2^p \left(\frac{x_1}{\alpha}, Q^2 = M^2 \right) \\ &\times \left\{ m_q^2 \alpha^4 \left[\frac{l_1}{(p_T^2 + \varepsilon^2)} - \frac{l_2}{4\varepsilon} \right] + \right. \\ &\left. + [1 + (1 - \alpha)^2] \left[\frac{\eta p_T l_3}{(p_T^2 + \varepsilon^2)} - \frac{l_1}{2} + \frac{\varepsilon l_2}{4} \right] \right\} \quad (17) \end{aligned}$$

where $\varepsilon = \alpha m_q$. The quantities $l_{1,2,3}$, are given by:

$$\begin{aligned} l_1 &= \int_0^\infty dr r J_0(p_T r) K_0(\varepsilon r) \sigma_{dip}(x_2, \alpha r) \\ l_2 &= \int_0^\infty dr r^2 J_0(p_T r) K_1(\varepsilon r) \sigma_{dip}(x_2, \alpha r) \\ l_3 &= \int_0^\infty dr r J_1(p_T r) K_1(\varepsilon r) \sigma_{dip}(x_2, \alpha r) \end{aligned} \quad (18)$$

GBW Dipole Cross Section

If we consider that the cross section is dominated by small dipoles, we use the GBW (Golec - Biernat e Wusthoff) parameterization and taking the small r limit, then calculate analytically the integrals (18).

$$\sigma_{dip}(x, \vec{r}; \gamma) = \sigma_0 \left[1 - \exp \left(-\frac{r^2 Q_{sat}^2}{4} \right)^{\gamma_{eff}} \right], \quad (19)$$

$\gamma_{eff} = 1$ and the remaining parameters are fitted to DIS HERA data at small x . The saturation scale is defined as $Q_{sat}^2(x) = \left(\frac{x_0}{x} \right)^\lambda$.

This dipole cross-section decreases over short distances $\propto p_T^2$ (color transparency) and saturates at large separations.

Taking the approach $\sigma_{dip} \approx \sigma_0(r^2 Q_{sat}^2)$, in the region in which $p_T \gg Q_{sat}$, we have:

$$I_1 = \sigma_0 Q_{sat}^2 \frac{(\varepsilon^2 - p_T^2)}{(p_T^2 + \varepsilon^2)^3}$$

$$I_2 = \sigma_0 Q_{sat}^2 \frac{4\varepsilon(\varepsilon^2 - 2p_T^2)}{(p_T^2 + \varepsilon^2)^4}$$

$$I_3 = \sigma_0 Q_{sat}^2 \frac{2p_T \varepsilon}{(p_T^2 + \varepsilon^2)^3}$$

The CGC dipole cross section is parameterized as:

$$\sigma_{dip}(x, r) = \sigma_0 \begin{cases} \mathcal{N}_0 \left(\frac{\bar{\tau}^2}{4} \right) \gamma_{\text{eff}}(x, r), & \text{for } \bar{\tau} \leq 2, \\ 1 - \exp \left[-a \ln^2 (b \bar{\tau}) \right], & \text{for } \bar{\tau} > 2, \end{cases}$$

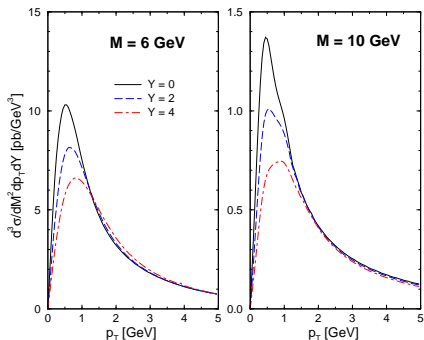
where $\bar{\tau} = rQ_{\text{sat}}(x)$

For the color transparency region near saturation border ($\bar{\tau} \leq 2$), the behavior is driven by

$$\gamma_{\text{eff}}(x, r) = \gamma_{\text{sat}} + \frac{\ln(2/\bar{\tau})}{\kappa \lambda \mathbf{y}}, \text{ where } \gamma_{\text{sat}} = 0.63.$$

Results

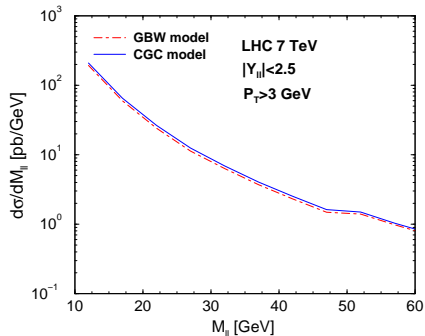
Differential cross section of dileptons



- The p_T spectrum is quite sensitive to the particular model of dipole cross section;
- The large rapidity cases give smaller cross sections;
- The peak on the distributions is shifted to larger values on p_T ;
- The peak is located at momentum around $p_T \approx 1$.

Figure: Low mass DY differential cross sections, $d^3\sigma/dM^2 dY dp_T$, as a function of dilepton transverse momentum, p_T , at energy of $\sqrt{s} = 7$ TeV, using the GBW model for the dipole cross section.

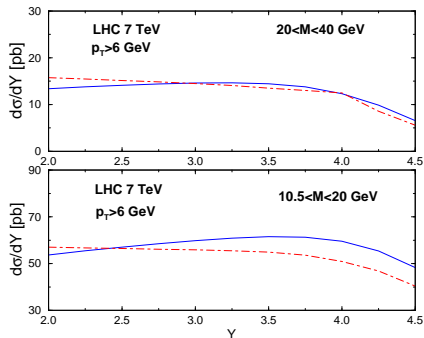
Dilepton invariant mass distribution



- GBW model (dot-dashed line), CGC model (solid line);
- The mass deviation between these two models occurs at large p_T ;
- Distinct p_T cuts will lead to a different overall normalization for the invariant mass distribution;
- ATLAS cuts: $12 < M_{\ell\ell} < 66 \text{ GeV}$, $p_T > 3 \text{ GeV}$, $|y| < 2.5$.

Figure: Invariant mass distribution in the range $12 < M_{\ell\ell} < 66 \text{ GeV}$. The imposed cuts at energy of $\sqrt{s} = 7 \text{ TeV}$ are lepton pair rapidities $|Y_{\ell\ell}| < 2.5$ and dilepton transverse momentum $p_T \geq 3 \text{ GeV}$.

Forward dilepton rapidity distribution



- GBW model(dot-dashed line), CGC model(solid line);
- $\mu^2 = \frac{1}{2}[(1-x_1)M^2 + p_T^2]$;
- The rapidity distribution is sensitive to the hard scale;
- LHCb cuts: $20 < M_{ll} < 40$ GeV,
 $10.5 < M_{ll} < 20$ GeV, $p_T^\mu > 6$ GeV;
- In the forward rapiditys: $0.6, \leq \langle Q_{sat}^2 \rangle \leq 1.2$ for
 $\langle M_{ll} \rangle \simeq 15.25$ GeV.

Figure: The dilepton rapidity distribution at $\sqrt{s} = 7$ TeV imposing the cut on dilepton transverse momentum $p_T > 6$ GeV and two invariant mass regions: (upper plot) $20 \leq M_{\ell\ell} \leq 40$ GeV and (lower plot) $10.5 \leq M_{\ell\ell} \leq 20$ GeV.

- Low mass DY production can be addressed in the color dipole picture without any free parameters by using dipole cross section determined from current phenomenology in DIS;
- The saturation effects play a significant role for the measured range of p_T at the LHC even at midrapidities as the saturation scale is enhanced by a sizable factor in comparison with the RHIC;
- The rapidity distribution of the DY production is sensitive to the chosen hard scale as also occurs for the LO pQCD approach;
- The rapidity distribution is driven by the effective anomalous dimension, with is distinct for each model;
- The considered cuts were motivated by LHCb and ATLAS analysis for low mass Drell Yan.

Thank you!